

## **SULFUR OXIDE ADSORBENTS AND EMISSIONS CONTROL**

### **GOVERNMENT RIGHTS**

This invention was made with Government support under Contract Number DE-  
5 AC06-76RLO1830 awarded by the U.S. Department of Energy. The Government has  
certain rights in the invention.

### **TECHNICAL FIELD**

The present invention is generally related to pollution control, and more  
10 particularly, but not exclusively, is directed to high capacity sulfur oxide adsorbents and  
uses therefore in emissions control.

### **BACKGROUND**

The combustion waste gases (i.e. the exhaust) of thermal power plants, factories,  
15 on-road vehicles, diesel generators, and the like contain  $\text{SO}_x$  and  $\text{NO}_x$ . State and federal  
regulations limit the permissible amounts of these emissions because they create  
environment problems, such as acid rain. Accordingly, there is a continual need for  
improvements in the cost effective and efficient control of these emissions.

One mechanism for limiting  $\text{NO}_x$  and  $\text{SO}_x$  emissions is to remove or scrub the  
20 pollutants from the exhaust gas using an absorption bed, trap or similar device. Because  
many  $\text{NO}_x$  traps have been found to be poisoned by the presence of  $\text{SO}_x$ , it is important to

remove as much  $\text{SO}_x$  from the exhaust gas as possible. However, as compared to the large volume of studies on  $\text{NO}_x$  reduction, sulfur oxide removal using solid adsorbents is an area in need of scientific advancement. For example, certain types of materials have been identified as possible solid adsorbents for use in a  $\text{SO}_x$  adsorption bed or traps, for example calcium oxide and alkalized alumina ( $\text{Na}/\text{Al}_2\text{O}_3$  or  $\text{K}/\text{Al}_2\text{O}_3$ ), copper-based adsorbents, e.g.  $\text{Cu}/\text{Al}_2\text{O}_3$ , promoted metal oxides, e.g.  $\text{TiO}_2$ ,  $\text{Al}_2\text{O}_3$ ,  $\text{ZrO}_2$ , promoted cerium oxide (La- or Cu- doped  $\text{CeO}_2$ ), and supported cobalt ( $\text{Co}/\text{Al}_2\text{O}_3$ ). Unfortunately, over the temperature range of about  $250^\circ\text{C}$  to  $475^\circ\text{C}$ , these materials typically have a relatively low absorption capacity. For example, their total adsorption capacity of  $\text{SO}_2$  is typically less than about 10 wt% based on the weight of the absorbent, and their breakthrough absorption capacity can be substantially lower, depending on operating conditions. As it is combustion in this temperature range that leads to a significant portion of the total  $\text{SO}_x$  emissions, a greater adsorption capacity at these temperatures is needed.

One approach to increasing the absorption capacity of  $\text{SO}_x$  absorption beds is to provide an oxidation catalyst upstream or admixed with the bed so as to convert most of the  $\text{SO}_2$  to  $\text{SO}_3$ , since  $\text{SO}_3$  is generally more readily adsorbed than  $\text{SO}_2$  due to its formation of stable surface sulfates. However, the cost of recovery of the oxidation catalyst (frequency a precious metal) and the relatively poor conversion efficiency of  $\text{SO}_2$  to  $\text{SO}_3$  at temperatures below about  $300^\circ\text{C}$  limits the effectiveness of this approach as well.

Accordingly, there is a need for solid SO<sub>x</sub> absorbents with high absorption capacity at lower temperatures and which reduce or eliminate the need for separate oxidation catalysts. In one aspect the present invention addresses this need and provides a major improvement to SO<sub>x</sub> absorption for emissions control.

## SUMMARY

The present invention provides systems and techniques for SO<sub>x</sub> emission control. While the actual nature of the invention covered herein can only be determined with reference to the claims appended hereto, certain aspects of the invention that are  
5 characteristic of the embodiments disclosed herein are described briefly as follows.

In one form, the invention concerns materials for absorbing, trapping, or otherwise eliminating oxides of sulfur from gases, for example those sulfur oxides present in exhaust gases of internal combustion engines. The materials are mixed oxides having a framework of metal cations M each surrounded by 6 oxygen atoms  
10 wherein the octahedra (MO<sub>6</sub>) thus formed are connected together by edges and vertices generating a structure that produces channels in at least one direction in space. The sides of these channels are formed by linking the octahedra (MO<sub>6</sub>), which connect together by the edges, these sides connecting themselves together via the vertices of the octahedra. Thus, the width of the channels can vary depending on whether the  
15 sides are composed of 2, 3 and/or 4 octahedra (MO<sub>6</sub>), which in turn depends on the mode of preparation. This type of material is known by its acronym OMS, Octahedral Molecular Sieve. In accordance with one form of the invention, the materials are selected so that they have a structure that generates channels either with a square cross section composed of, for example, one octahedra by one octahedra (OMS 1 x 1), two  
20 octahedra by two octahedra (OMS 2 x 2) or three octahedra by three octahedra (OMS 3 x 3), or with a rectangular cross section composed of, for example, two octahedra by

three octahedra (OMS 2 x 3). Thus, certain of the materials will have a pyrolusite (OMS 1 x 1), hollandite (OMS 2 x 2), romanechite (OMS 2 x 3) or todorokite (OMS 3 x 3) type structure. Other OMS structures, such as 1x3, 1x4 or 2x4, 3x4 or 4x4, are also contemplated, though the 2x2 structure has been found to be particularly effective in certain applications.

The OMS materials of the present invention are preferably manganese based (Mn-OMS), which means that a major portion of the metal cation M is manganese (Mn). An element is in the majority when it satisfies the following formula:

$(n_{\text{maj}}/\sum n_{\text{M}}) > 1/N$ , where  $n_{\text{M}}$  is the number of atoms of element (M) and N is the number

of different elements (M) composing the framework,  $n_{\text{maj}}$  being the highest number of atoms of element (M). Most preferably, over 50% of the elements M are manganese for example at least 75% or at least 90% of the element M by mole. Preferably the manganese has an oxidation number between +2 and +4. The balance of element M can include one or more elements from groups IIIB to IIIA in the periodic table such as  $\text{Zn}^{2+}$ ,  $\text{Co}^{2+}$ ,  $\text{Ni}^{2+}$ ,  $\text{Fe}^{2+}$ ,  $\text{Al}^{3+}$ ,  $\text{Ga}^{3+}$ ,  $\text{Fe}^{3+}$ ,  $\text{Ti}^{3+}$ ,  $\text{In}^{3+}$ ,  $\text{Cr}^{3+}$ ,  $\text{Si}^{4+}$ ,  $\text{Ge}^{4+}$ ,  $\text{Ti}^{4+}$ ,  $\text{Sn}^{4+}$ , and  $\text{Sb}^{5+}$  and combinations thereof. The material used in this invention has a characteristic structure of high surface area and may be capable of oxidizing  $\text{SO}_2$  to  $\text{SO}_3$  and converting  $\text{SO}_3$  to a sulfate. In certain cases, but not all cases, another cation, such as  $\text{H}^+$ ,  $\text{NH}_4^+$ ,  $\text{Li}^+$ ,  $\text{Na}^+$ ,  $\text{Ag}^+$ ,  $\text{K}^+$ ,  $\text{Rb}^+$ ,  $\text{Tl}^+$ ,  $\text{Cs}^+$ ,  $\text{Mg}^{2+}$ ,  $\text{Ca}^{2+}$ ,  $\text{Sr}^{2+}$ ,  $\text{Ba}^{2+}$ ,  $\text{Ra}^{2+}$ ,  $\text{Cu}^{2+}$ ,  $\text{Pb}^{2+}$ , locates in the channels in the OMS structures.

The absorbing phase of materials with type OMS 2\*2, OMS 2\*3 and OMS 3\*3 of one aspect of the invention has a three-dimensional structure that generates channels in at least one direction in space, is composed of octahedra ( $\text{MO}_6$ ) and comprises:

5                   at least one element (M) selected from the group formed by elements from groups IIIB, IVB, VB, VIB, VIIB, VIII, IB, IIB, IIIA of the periodic table and germanium, each element M being coordinated with 6 oxygen atoms, and located at the center of the oxygen octahedra, wherein a major portion of M is manganese; and

10                   at least one element (B) selected from the group formed by the alkali elements IA, the alkaline-earth elements IIA, the rare earths IIIB, transition metals or elements from groups IIIA and IVA, element B generally being located in channels in the oxide structure.

More particularly, elements M are selected from scandium, titanium,  
15   zirconium, vanadium, niobium, chromium, molybdenum, tungsten, manganese, iron, cobalt, nickel, copper, zinc, aluminum, gallium, and mixtures thereof.

The average charge (oxidation number) carried by the cation or cations M from groups IIIB to IIIA is preferably about +3.5 to +4. Preferably, at least about 50% of the elements (M) in the material are manganese, titanium, chromium, aluminum, zinc,  
20   copper, zirconium, iron, cobalt, and/or nickel. More preferably, over 50% of the elements (M) are manganese, chromium, copper, iron, titanium and/or zirconium. In

one form, manganese composes at least about 50% of the M element by mole, for example at least 75% or 90% of the M element.

Other elements M from groups IIIB to IIIA can be added in minor quantities as dopants. Preferably, the elements from groups IIIB to IIIA added in minor quantities  
5 are selected from scandium, titanium, zirconium, vanadium, niobium, chromium, molybdenum, tungsten, manganese, iron, cobalt, nickel, copper, zinc, aluminum, gallium, and mixtures thereof.

Elements (B) belong to the group formed by the alkali elements IA, alkaline-earth elements IIA, rare earth elements IIIB, transition metals and elements from  
10 groups IIIA and IVA. They are located in the channels of the material. Preferably, metal B is selected from the group formed by potassium, sodium, magnesium, barium, strontium, iron, copper, zinc, aluminum, rubidium and calcium and mixtures thereof.

A number of different methods exist for preparing these materials (see references 3 and 4 below, for example). They may be synthesized by mixing and  
15 grinding solid inorganic precursors of metal oxides (metals M and B), followed by calcining. The materials can also be obtained by heating solutions of precursor salts to reflux, drying and calcining, by precipitating precursor salts by the sol-gel method, or by hydrothermal synthesis which consists of heating an aqueous solution containing the elements constituting the final material under autogenous pressure. The materials  
20 obtained from these syntheses can be modified by ion exchange or isomorphous substitution.

Optional metal (C) is introduced using any of the methods known to the skilled person: excess impregnation, dry impregnation, ion exchange, etc.

The material of the invention generally has a specific surface area in the range 1 to 300 m<sup>2</sup>/g, preferably in the range 2 to 300 m<sup>2</sup>/g, and more preferably in the range 30 to 250 m<sup>2</sup>/g. The adsorption kinetics are better when the specific surface area is high, i.e., in the range 10 m<sup>2</sup>/g such as in the range 30 to 250 m<sup>2</sup>/g.

The sorbent phase can be in the form of a powder, beads, pellets or extrudates; they can also be deposited or directly prepared on monolithic supports of ceramic or metal. To increase the dispersion of the materials and thus to increase their absorption capacity, the materials can be deposited on porous supports with a high specific surface area before being formed (extrusion, coating . . . ). These supports are generally selected from the group formed by the following compounds: alumina (alpha, beta, delta, gamma, khi, or theta alumina), silicas (SiO<sub>2</sub>), silica-aluminas, zeolites, titanium oxide (TiO<sub>2</sub>), zirconium oxide (ZrO<sub>2</sub>), magnesium oxide (MgO), divided carbides, for example silicon carbides (SiC), used alone or as a mixture. Mixed oxides or solid solutions comprising at least two of the above oxides can be added.

For many uses, such as in connection with a vehicle exhaust, it is usually preferable to use rigid supports (monoliths) with a large open porosity (more than 70%) to limit pressure drops that may cause high gas flow rates, and in particular high exhaust gas space velocities. These pressure drops are deleterious to proper



functioning of the engine and contribute to reducing the efficiency of an internal combustion engine (gasoline or diesel). Further, the exhaust system is subjected to vibrations and to substantial mechanical and thermal shocks, so catalysts in the form of beads, pellets or extrudates run the risk of deterioration due to wear or fracturing.

5 Two techniques are used to prepare the catalysts of the invention on monolithic ceramic or metal supports (or substrates).

The first technique comprises direct deposition on the monolithic support, using a wash coating technique which is known to the skilled person, to coat the adsorbing phase prepared using the operating procedure described, for example, in reference (4)  
10 below. (S. L. Suib, C-L O'Young, "Synthesis of Porous Materials", M. L. Occelli, H. Kessler, eds, M. Dekker, Inc., p. 215, 1997). The adsorbent phase can be coated just after the co-precipitation step, hydrothermal synthesis step or heating under reflux step, the final calcining step being carried out on the phase deposited on the monolith, or the monolith can be coated after the material has been prepared in its final state, i.e.,  
15 after the final calcining step.

The second technique comprises depositing the inorganic oxide on the monolithic support and then calcining the monolith between 500°C and 1100°C so that the specific surface area of this oxide is in the range 20 to 150 m<sup>2</sup>/g, then coating the monolithic substrate covered with the inorganic oxide with the adsorbent phase  
20 obtained after the steps described in the reference (4).

Monolithic supports that can be used include: ceramics, where the principal elements can be alumina, zirconia, cordierite, mullite, silica, alumino-silicates or a combination of several of these compounds; a silicon carbide and/or nitride; an aluminium titanate; and/or a metal, generally obtained from iron, chromium or  
5 aluminium alloys optionally doped with nickel, cobalt, cerium or yttrium.

The structure of a ceramic supports can be that of a honeycomb, or they are in the form of a foam or fibers.

Metal supports can be produced by winding corrugated strips or by stacking corrugated sheets to constitute a honeycomb structure with straight or zigzag channels  
10 which may or may not communicate with each other. They can also be produced from metal fibers or wires which are interlocked, woven or braided.

With supports of metal comprising aluminum in their composition, it is recommended that they are pre-treated at high temperature (for example between 700°C and 1100°C) to develop a micro-layer of refractory alumina on the surface. This  
15 superficial micro-layer, with a porosity and specific surface area which is higher than that of the original metal, encourages adhesion of the active phase and protects the remainder of the support against corrosion.

The quantity of sorbent phase deposited or prepared directly on a ceramic or metallic support (or substrate) is generally in the range 20 to 300 g per liter of said  
20 support, advantageously in the range 50 to 200 g per liter.

The materials of the invention can thus adsorb oxides of sulfur present in the gases, in particular exhaust gases. These materials are capable of adsorbing  $\text{SO}_x$  at a temperature which is generally in the range  $50^\circ\text{C}$  to  $650^\circ\text{C}$ , preferably in the range  $100^\circ\text{C}$  to  $600^\circ\text{C}$ , more preferably in the range  $150^\circ\text{C}$  to  $550^\circ\text{C}$ .

5 For diesel engines in automobiles, an intended application, the temperature of the exhaust gas may be in the range  $150^\circ\text{C}$  to  $500^\circ\text{C}$  and rarely exceeds  $600^\circ\text{C}$ . The materials used in the process of the invention are thus suitable for sorbing oxides of sulfur present in the exhaust gases of stationary engines or, particularly, automotive diesel engines or spark ignition (lean burn) engines, but also in the gases from gas  
10 turbines operating with gas or liquid fuels. These exhaust gases typically contain oxides of sulfur in the range of a few tens to a few thousands of parts per million (ppm) and can contain comparable amounts of reducing compounds ( $\text{CO}$ ,  $\text{H}_2$ , hydrocarbons) and nitrogen oxides. These exhaust gases might also contain larger quantities of oxygen (1% to close to 20% by volume) and steam, though the present  
15 sorbents can be effective in oxygen free environments as well. The sorbent material of the invention can be used with HSVs (hourly space velocity, corresponding to the ratio of the volume of the monolith to the gas flow rate) for the exhaust gas generally in the range  $500$  to  $150,000\text{ h}^{-1}$ , for example in the range  $5,000$  to  $100,000\text{ h}^{-1}$ .

In has been found that absorption of  $\text{SO}_x$  leads to a noticeable color change in  
20 the sorbent. Accordingly, in one variation, a  $\text{SO}_x$  trap is provided by a quantity of the sorbent contained in a housing having a window. The color of the sorbent material is

periodically monitored through the window with the need to replace or recharge the trap indicated by the color change. In this or other refinements, a spent SO<sub>x</sub> trap can be regenerated by appropriate reflux synthesis so as to reuse the sorbent support and the housing.

5           The SO<sub>x</sub> sorbent material of the present invention can be used anywhere SO<sub>x</sub> needs to be absorbed. It has been found that significant advantages can be realized in the overall control of emissions from a combustion exhaust by locating the SO<sub>x</sub> sorbent material upstream from a particulate filter or NO<sub>x</sub> trap.

          According to another aspect of the invention, SO<sub>x</sub> adsorption is provided by a  
10   manganese oxide material which has inherent oxidizing capability, so that SO<sub>2</sub> can be oxidized and absorbed without use of a separate and costly oxidation catalyst, and which has a high total absorption capacity, for example greater than about 40% by weight, thereby providing economical and efficient emissions control.

## BRIEF DESCRIPTION OF THE FIGURES

Although the characteristic features of this invention will be particularly pointed out in the claims, the invention itself, and the manner in which it may be made and used, may be better understood by referring to the following description taken in connection with the accompanying figures forming a part thereof.

FIG. 1 is exemplary plots of the absorption of  $\text{SO}_2$  on 2x2 Mn-OMS materials and on  $\text{MnO}_2$ .

FIGS. 2a and 2b are exemplary scanning electron microscopy images of a 2x2 Mn-OMS material before and after  $\text{SO}_2$  absorption, respectively.

FIGS. 3a and 3b are exemplary x-ray diffraction patterns of a 2x2 Mn-OMS material before and after  $\text{SO}_2$  adsorption, respectively.

FIG. 4 is exemplary plots of absorption of  $\text{SO}_2$  on an Mn-OMS material at different gas feed temperatures.

FIG. 5 is exemplary plots of adsorption of  $\text{SO}_2$  on an Mn-OMS material at different gas feed rates.

FIG. 6 is exemplary plots of adsorption of  $\text{SO}_2$  on an Mn-OMS material at different concentrations of  $\text{SO}_2$  in the feed gas.

FIG. 7 is exemplary plots of absorption of  $\text{SO}_2$  on an Mn-OMS material at different feed gas compositions.

FIG. 8 is exemplary plots of absorption of  $\text{SO}_2$  on 2x3 Mn-OMS materials at different gas feed rates.

FIG. 9 is exemplary plots of absorption of  $\text{SO}_2$  on a 2x4 Mn-OMS material.

FIG. 10 is a schematic illustration of an emissions control system implemented on a vehicle producing combustion exhaust according to an embodiment of the invention.

5        FIG. 11 is a perspective view of a  $\text{SO}_x$  filter having a monitoring window and regeneration ports according to an embodiment of the invention.

## DESCRIPTION OF THE ILLUSTRATED EMBODIMENT

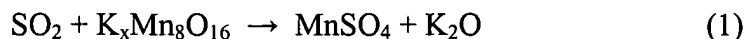
For the purposes of promoting an understanding of the principles of the invention, reference will now be made to the embodiments illustrated in the drawings and specific language will be used to describe the same. It will nevertheless be understood that no limitation of the scope of the invention is hereby intended.

Alterations and further modifications in the illustrated devices, and such further applications of the principles of the invention as illustrated herein are contemplated as would normally occur to one skilled in the art to which the invention relates.

In one form, the present invention employs a manganese based octahedral molecular sieve as a high capacity sulfur oxide solid absorbent. As compared to other adsorbents studied for the removal of SO<sub>2</sub> from waste gases, this material provides surprising high capacity and efficiency. In a preferred form, this material is referred to as Mn-OMS 2x2.

The basic structure of the materials employed in the Examples that follow consists of MnO<sub>6</sub> octahedra joined at edges to form a 2 x 2 hollandite tunnel structure with a pore size of about 0.46 nm. (1) For cryptomelane, a counter-cation, K<sup>+</sup>, is present within the tunnel structure for charge compensation. Mn can assume an oxidation state of 4+, 3+, or 2+, and the average Mn oxidation state can be controlled within a certain range during synthesis. Generally, this material has a high surface area (~ 80 m<sup>2</sup>/g), and high redox reaction activity. (2)

Without intending to be bound by any theory of operation, the present invention is based on carrying out the following reaction:



5

$\text{SO}_2$  is oxidized to  $\text{SO}_3$  by  $\text{Mn}^{4+}$  and  $\text{Mn}^{3+}$ , and  $\text{Mn}^{4+}$  and  $\text{Mn}^{3+}$  are simultaneously reduced to  $\text{Mn}^{2+}$  ( $\text{MnO}$ ). The  $\text{SO}_3$  produced then reacts with  $\text{Mn}^{2+}$  to form  $\text{MnSO}_4$ .

As explained herein, tunnel structure cryptomelane was found to be a high capacity sulfur dioxide adsorbent. Its  $\text{SO}_2$  capacity from  $250^\circ\text{C}$  to  $475^\circ\text{C}$  is more than ten times  
10 higher than that of conventional  $\text{SO}_2$  adsorbents. Its maximum  $\text{SO}_2$  capacity can be as high as about 74 wt%. The dominant mechanism for  $\text{SO}_2$  absorption is believed to be that  $\text{SO}_2$  is oxidized by  $\text{Mn}^{4+}$  and  $\text{Mn}^{3+}$  to  $\text{SO}_3$ , with the  $\text{SO}_3$  reacting with the co-produced  $\text{Mn}^{2+}$  to form  $\text{MnSO}_4$ . It has been found that this reaction is primarily  
15 controlled by the mass diffusion of  $\text{SO}_2$  through the adsorbent, and that it can surprisingly effectively occur in an oxygen-free environment. In addition, the visibly significant color change of cryptomelane from black to yellow after  $\text{SO}_2$  absorption can be used as a convenient indicator for the adsorbent replacement.

Cryptomelane for  $\text{SO}_2$  absorption can be synthesized either from a mixture of  $\text{KMnO}_4$  and  $\text{MnSO}_4$  or a mixture of  $\text{MnSO}_4$  and  $\text{KOH}$  solution. After  $\text{SO}_2$  absorption,  
20  $\text{MnSO}_4$  is formed, which can subsequently be dissolved in water and used as raw material for a subsequent cryptomelane synthesis. To regenerate the  $\text{SO}_2$  absorption trap,



therefore, only KOH and O<sub>2</sub> is needed because the adsorbent support (such as a monolith) and the MnSO<sub>4</sub> can be re-used.

This highly efficient SO<sub>2</sub> adsorbent can be used for removal of SO<sub>2</sub> generated from thermal power plants, factories, and on-road vehicles. It can be especially effective for  
5 removal of SO<sub>x</sub> that is present in the emissions of diesel trucks, in order to protect downstream emissions control devices such as particulate filters and NO<sub>x</sub> traps that are poisoned by SO<sub>x</sub>.

Turning now to FIG. 10, a vehicle 20 implementing a simplified emissions control system according to the present invention is depicted. Vehicle 20 has an engine 22  
10 fluidly connected to upstream and a downstream emissions control devices 24 and 26 respectively. Devices 24 and 26 perform different emissions control functions, and while they could be combined into a single device, as described more fully below, certain problems are avoided by the provision of separate devices.

The exhaust 21 from the engine 22 is first fed to the upstream device 24. The  
15 transfer of the exhaust, and all other fluid transfer operation can be in any conventional fashion, such as the exhaust piping of a conventional automobile, and may include intermediate fluid processing operations, such as catalytic conversion, mixing with other gases, or recycling of exhaust to the engine.

The upstream device 24 is a SO<sub>x</sub> scrubber, whose function is to remove any sulfur  
20 oxides from the exhaust gas 21 and to prevent their passage via channel 25 to the downstream device 26 and eventually the exhaust 28 to the atmosphere. The SO<sub>x</sub>

scrubber functions to remove most if not all of any sulfur oxides in the gaseous exhaust

21. The SO<sub>x</sub> scrubber contains a solid SO<sub>x</sub> sorbent as described herein, preferably one supported on a monolith or similar support. The sorbent removes the SO<sub>x</sub> from the passing gas stream, for example by permanent or reversible sorption (adsorption or  
5 absorption) trapping, filtering, or chemical reaction therewith, and thereby prevents SO<sub>x</sub> from entering the downstream device 26.

The downstream device 26 provides a different emissions control function than the upstream device 24. As illustrated, the downstream device is a NO<sub>x</sub> scrubber or particulate filter and any conventional scrubber or filter can be employed. As many  
10 conventional NO<sub>x</sub> traps and/or particulate filters are fouled or poisoned by the presence of SO<sub>x</sub>, the provision of upstream device 24 inventively reduces or eliminates this possibility by providing an inlet stream to device 26 that is substantially SO<sub>x</sub> free. For example, it is contemplated that device 24 will function to cause fluid at 25 to have less than 1% of the SO<sub>x</sub> concentration in the exhaust 21, more preferably less than about  
15 0.1%.

Turning now to FIG. 11, an exemplary SO<sub>x</sub> scrubber 30, which can be employed for device 24 in the FIG. 10 system, is depicted. Scrubber 30 includes a housing 32 having a fluid inlet 34, a fluid outlet 36 and a fluid flow path therebetween. The housing contains a SO<sub>x</sub> sorbent in the flow path so as to facilitate the removal of SO<sub>x</sub> from the  
20 fluid as it passes through the SO<sub>x</sub> scrubber. Housing 32 also contains a window 38 providing visual access to the sorbent contained therein. As the sorbent contained in the

housing 32 absorbs the  $\text{SO}_x$ , it will undergo a noticeable color change, with the sorbent nearer the inlet 34 becoming saturated (and thus changing color) sooner than the sorbent near the outlet 36. The resulting transition between different colored portions of the sorbent provides an indication on the extent that the sorbent packing has becoming spent.

5 Accordingly, a series of indicator marks 39 are provided on the window 38 or on the housing 32 adjacent the window 38 for measuring the remaining sorption capacity of the scrubber 30. For example, during routine maintenance of a machine on which scrubber 30 is implemented, vehicle 20 for example, the window 38 can be checked to determine whether replacement of the scrubber 30 is necessary.

10 When replacement is needed, i.e. the sorbent is saturated and entirely changed colors, the scrubber 30 can simply be removed from the exhaust stream and replaced. In another form of the invention, once removed, the spent sorbent and/or the scrubber 30 can be reused. For example when the spent sorbent is converted to  $\text{MnSO}_4$ , this  $\text{MnSO}_4$  can be used as a starting material to reform the Mn-OMS material on the support. This reforming can be accomplished by removing the spent sorbent and its support (such as a monolith) from the housing 32. After processing and appropriate calcination the spent sorbent is returned to its OMS structure and is ready to absorb additional  $\text{SO}_x$ .

Alternatively, the necessary reagents for reforming the spent sorbent, for example KOH and  $\text{O}_2$ , can be circulated through the housing 32 without removing the spent sorbent. The inlet and outlet ports 34 and 36 can be used as the reagent inlet and outlet ports to recharge the sorbent in this fashion when the scrubber 30 is removed from the

exhaust stream. However, as illustrated, scrubber 30 includes optional dedicated inlet and outlet ports 44 and 42 for this purpose. Ports 42, 44 permit recharging without removal from the exhaust, or they may be used in conjunction with offline recharging via inlet and outlet 34, 36.

5           Reference will now be made to examples illustrating specific features of inventive embodiments. It is to be understood, however, that these examples are provided for illustration and that no limitation to the scope of the invention is intended thereby. Further, certain observations, hypotheses, and theories of operation are presented in light of these examples in order to further understanding, but these are likewise not intended to  
10       limit the scope of the invention.

## EXAMPLES

### EXAMPLE 1

#### SAMPLE PREPARATIONS AND TEST CONDITIONS OMS 2X2

15           2x2 manganese based octahedral molecular sieve (tunnel structure cryptomelane) was prepared using the methods developed by DeGuzman, et al. (3) A typical synthesis was carried out as follows: 11.78 g  $\text{KMnO}_4$  in 200 ml of water was added to a solution of 23.2 g  $\text{MnSO}_4 \cdot 4\text{H}_2\text{O}$  in 60 ml of water and 6 ml of concentrated  $\text{HNO}_3$ . The solution was  
20       refluxed at  $100^\circ\text{C}$  for 24 h, and the product was washed and dried at  $120^\circ\text{C}$ . Hydrothermal reaction in Teflon bottles at  $90^\circ\text{C}$ , instead of the reflux method, was also used for the synthesis.

An alternative synthesis method for cryptomelane was purging O<sub>2</sub> through mixture of MnSO<sub>4</sub> and KOH solution, followed by calcination at 600°C. (3) A typical preparation was: a solution of 15.7 g KOH in cold 100 ml of water was added to a solution of 14.9 g of MnSO<sub>4</sub>·H<sub>2</sub>O in 100 ml of water. Oxygen gas was bubbled (about 10 L/min) through  
5 the solution for 4 hours. The product was washed with water and calcined in air for 20 h.

The dried materials were sieved to provide 40 – 80 mesh particles for the SO<sub>2</sub> absorption tests, which was carried out in a temperature controlled reactor with a Sulfur Chemiluminescent Detector (SCD) analysis system. Unless otherwise stated, the absorption testing conditions were 0.5 gram 40-80 mesh absorbent particles, 100 standard  
10 cubic centimeters per minute (sccm) exhaust air flow with 250 parts per million (ppm) SO<sub>2</sub>, 75% N<sub>2</sub>, 12% O<sub>2</sub>, and 13% CO<sub>2</sub>.

The SO<sub>2</sub> absorption performance of cryptomelane material synthesized by refluxing mixture of KMnO<sub>4</sub> and MnSO<sub>4</sub> solutions was also systemically tested under different temperature, gas hour space velocity (GHSV), SO<sub>2</sub> concentrations, and feed gas  
15 compositions, and the results are summarized in Table 1.

Before each SO<sub>2</sub> absorption measurement, the material was heated at 500°C for 2 h in flowing air. To characterize the property changes before and after SO<sub>2</sub> absorption, powder X-ray diffraction pattern (XRD), particle surface area (SA), and scanning electron microscopy (SEM) images were collected on some of the tested materials.

Table 1  
SO<sub>2</sub> absorption test conditions for cryptomelane material

Variable conditions	Other conditions
SO <sub>2</sub> absorption temperature 250°C, 325°C, and 475°C	0.5 g 40-80 mesh absorbent, feed gas: 250 ppm SO <sub>2</sub> , 82% N <sub>2</sub> , 18% O <sub>2</sub> , ~ 8,000 hr <sup>-1</sup> GHSV
Gas Hour Space Velocity, GHSV, hr <sup>-1</sup> 8000, 30000, and 60000	0.5 g 40-80 mesh absorbent for 8K and 30K hr <sup>-1</sup> GHSV test, and 0.25 g for 60K test, 325°C, feed gas: 250 ppm SO <sub>2</sub> , 82% N <sub>2</sub> , 18% O <sub>2</sub>
SO <sub>2</sub> concentration in feed gas 50 ppm and 250 ppm	0.5 g 40-80 mesh absorbent for 250 ppm SO <sub>2</sub> test, and 0.25 g for 50 ppm test 325°C, feed gas: 82% N <sub>2</sub> , 18% O <sub>2</sub> , ~30000 hr <sup>-1</sup> GHSV,
Feed gas composition Air (250 ppm SO <sub>2</sub> , 82% N <sub>2</sub> and 18% O <sub>2</sub> ) CO <sub>2</sub> effect (250 ppm SO <sub>2</sub> , 75% N <sub>2</sub> , 12% O <sub>2</sub> , and 13% CO <sub>2</sub> ) NO effect (178 ppm SO <sub>2</sub> , 178 ppm NO, 9% N <sub>2</sub> , 20% O <sub>2</sub> , 71% He) CO effect (250 ppm SO <sub>2</sub> , 250 ppm CO, 87% N <sub>2</sub> , 13% O <sub>2</sub> ) CO-NO-H <sub>2</sub> O effect (125 ppm SO <sub>2</sub> , 125 ppm CO, 125 ppm NO, 11% H <sub>2</sub> O*, 19% N <sub>2</sub> , 20% O <sub>2</sub> , 50% He) O <sub>2</sub> -free effect (250 ppm SO <sub>2</sub> , 12.5% N <sub>2</sub> , and 87.5% He)	For CO-NO-H <sub>2</sub> O test 0.25 g 40-80 mesh adsorbent, 325°C, 17K hr <sup>-1</sup> GHSV  For others 0.5 g 40-80 mesh adsorbent, 325°C, ~8K hr <sup>-1</sup> GHSV

\* Steam was introduced by purging O<sub>2</sub> through flask containing temperature-controlled de-ionized water. After passing through the absorbent, steam was removed before SCD detector using MD Gas Dryer (from Perma Pure Inc.) which can selectively separate H<sub>2</sub>O from gases mixture.

## EXAMPLE 2 (COMPARATIVE) COMPARATIVE BREAKTHROUGH ABSORPTION CAPACITIES

For purposes of comparison, SO<sub>2</sub> absorption capability of several commercially available materials were tested at a temperature range from 250°C to 475°C under the testing conditions indicated above (0.5 gram 40-80 mesh absorbent particles, 100 sccm exhaust air flow with 250 ppm SO<sub>2</sub>, 75% N<sub>2</sub>, 12% O<sub>2</sub>, and 13% CO<sub>2</sub>). These materials

included  $\text{La}_2\text{O}_3$  or  $\text{BaO}$  doped  $\text{ZrO}_2\text{-CeO}_2$  mixtures (from Daiichi Kigenso Kagaku Kogyo Co., Ltd.),  $\text{ZrO}_2$  (from RC100, Inc.),  $\text{Al}_2\text{O}_3$  (from Engelhard, acidic),  $\text{CaO}$  (from Alfa Aesar Inc), and  $\text{MnO}_2$  (from Erachem Comilog, Inc.) which were obtained from their respective commercial sources.

Table 2 presents a summary of the SO<sub>2</sub> absorption capacities for certain of these SO<sub>2</sub> adsorbents. The SO<sub>2</sub> capacity was calculated based on weight of SO<sub>2</sub> adsorbed per gram of adsorbent when 1% of the initial SO<sub>2</sub> concentration was observed eluting from the absorbent bed. This is defined as the breakthrough absorption capacity. As seen in Table 2, the SO<sub>2</sub> breakthrough absorption capacities for these materials are generally less than 5 wt%. Of the other materials tested, the absorption capacities for the MnO<sub>2</sub> was selected for more direct comparison to the materials of Example 1 and are presented in the Examples below.

Table 2  
SO<sub>2</sub> breakthrough absorption capacity of conventional SO<sub>2</sub> adsorbents

Materials tested	200°C	325°C	400°C	475°C
73.8% ZrO <sub>2</sub> -26.2%CeO <sub>2</sub> mixed oxide SA 53.5 m <sup>2</sup> /g, 10000 hr <sup>-1</sup> GHSV		2.2 wt%	2.2 wt%	2.2 wt%
73.2% ZrO <sub>2</sub> , 1.75% La <sub>2</sub> O <sub>3</sub> , 5.22% Nd <sub>2</sub> O <sub>3</sub> ,and 19.9% CeO <sub>2</sub> mixed oxide SA 60.3 m <sup>2</sup> /g, 7236 hr <sup>-1</sup> GHSV		2.4 wt%	3.1 wt%	3.6 wt%
61.8% ZrO <sub>2</sub> , 29.4%CeO <sub>2</sub> , and 8.9% La <sub>2</sub> O <sub>3</sub> mixed oxide SA 69.1m <sup>2</sup> /g, 11400 hr <sup>-1</sup> GHSV	2.0 wt%	3.5 wt%	5.0 wt%	5.3 wt%
70.3% ZrO <sub>2</sub> , 4.0% BaO, and 25.8% CeO <sub>2</sub> mixed oxide SA 29.2 m <sup>2</sup> /g, ~ 10000hr <sup>-1</sup> GHSV		1.7 wt%	1.7 wt%	2.5 wt%
ZrO <sub>2</sub> , SA 95.7 m <sup>2</sup> /g, 10000 hr <sup>-1</sup> GHSV				2.2 wt%
Al <sub>2</sub> O <sub>3</sub> , Engelhard Corp. SA 150 m <sup>2</sup> /g, Acidic 7,281 hr <sup>-1</sup> GHSV		1.0 wt%		
CaO, SA 2.7 m <sup>2</sup> /g, ~10, 000 hr <sup>-1</sup> GHSV		<0.2 wt%	<0.2 wt%	<0.2 wt%

1. Other test conditions: 0.5 g 40-80 mesh absorbent, feed gas: 250 ppm SO<sub>2</sub>, 75% N<sub>2</sub>, 12% O<sub>2</sub>, and 13% CO<sub>2</sub>
2. SO<sub>2</sub> capacity based on gram of SO<sub>2</sub> adsorbed per gram of catalyst at 1% SO<sub>2</sub> breakthrough point

5

### EXAMPLE 3 BREAKTHROUGH ABSORPTION CAPACITIES

10 Table 3 gives the SO<sub>2</sub> breakthrough and total absorption capacities of the materials synthesized according to Example 1, K<sub>x</sub>Mn<sub>8</sub>O<sub>16</sub> A (reflux synthesis, with projected final average Mn oxidation state 3.5<sup>+</sup>), K<sub>x</sub>Mn<sub>8</sub>O<sub>16</sub> B (reflux synthesis, with projected final average Mn oxidation state 4<sup>+</sup>), Cu-doped K<sub>x</sub>Mn<sub>8</sub>O<sub>16</sub> B (hydrothermal synthesis, with projected final average Mn oxidation state 4<sup>+</sup>), and K<sub>x</sub>Mn<sub>8</sub>O<sub>16</sub> C (synthesized from

15 MnSO<sub>4</sub> and KOH). The projected final Mn oxidation state (PAOS) is calculated based on the relative amount of KMnO<sub>4</sub> and MnSO<sub>4</sub> in the starting solution, i.e. PAOS = (moles of KMnO<sub>4</sub> \* 7 + moles of MnSO<sub>4</sub> \* 2)/(moles of KMnO<sub>4</sub> + moles of MnSO<sub>4</sub> ).

Breakthrough capacities were measured at 1% breakthrough as described in Example 2, and total SO<sub>2</sub> absorption capacity was also measured with the values given in parentheses

20 in Table 3. For example, the breakthrough and maximum SO<sub>2</sub> absorption capacities for K<sub>x</sub>Mn<sub>8</sub>O<sub>16</sub> B are 58 wt% and 68 wt% respectively. Under similar reaction conditions, these materials have significantly higher breakthrough SO<sub>2</sub> absorption capacity than the conventional SO<sub>2</sub> adsorbents given in Table 2. To facilitate comparison, the results for the commercially obtained electrolytic MnO<sub>2</sub> (EMD, Erachem Comilog, Inc.) discussed

25 above are presented in Table 3.



Table 3  
SO<sub>2</sub> absorption capacity of cryptomelane materials synthesized

Materials tested	SA, m <sup>2</sup> /g	SO <sub>2</sub> breakthrough capacity (total capacity)
K <sub>x</sub> Mn <sub>8</sub> O <sub>16</sub> A, 14000 hr <sup>-1</sup> GHSV	51	28 (45) <sup>b</sup> wt%
Cu-doped K <sub>x</sub> Mn <sub>8</sub> O <sub>16</sub> B <sup>a</sup> , 9637 hr <sup>-1</sup> GHSV	88	57.5 (67) wt%
K <sub>x</sub> Mn <sub>8</sub> O <sub>16</sub> B, ~7500 hr <sup>-1</sup> GHSV	74	58 (68) wt%
K <sub>x</sub> Mn <sub>8</sub> O <sub>16</sub> C, ~8000 hr <sup>-1</sup> GHSV	32	48 (xx) wt%
EMD MnO <sub>2</sub> , 12000 hr <sup>-1</sup> GHSV	30	3.5 (9) wt%

\*Other test conditions: 0.5 g 40-80 mesh absorbent, 325°C, feed gas: 250 ppm SO<sub>2</sub>, 82% N<sub>2</sub>, and 18% O<sub>2</sub> for K<sub>x</sub>Mn<sub>8</sub>O<sub>16</sub> C, for others: 75% N<sub>2</sub>, 12% O<sub>2</sub>, and 13% CO<sub>2</sub>

<sup>a</sup>CuSO<sub>4</sub> was added in MnSO<sub>4</sub> solution.

<sup>b</sup>Data in parentheses are maximum SO<sub>2</sub> absorption capacities.

#### EXAMPLE 4 SO<sub>2</sub> ABSORPTION AT 325°C

FIG. 1 is a plots showing SO<sub>2</sub> absorption on K<sub>x</sub>Mn<sub>8</sub>O<sub>16</sub> A, B, Cu-doped K<sub>x</sub>Mn<sub>8</sub>O<sub>16</sub> B, and EMD MnO<sub>2</sub>, as a function of the weight percentage of SO<sub>2</sub> fed at 325°C. The left axis is the percentage of SO<sub>2</sub> not absorbed (i.e. that passed through the bed) and corresponds to the S-shaped curves. The right axis is the wt% SO<sub>2</sub> absorbed and corresponds to the curves whose slope is initially 1 at low feed amounts and then tends towards slope of zero at high feed amounts. All weight percentages are relative weight of absorbent.

#### EXAMPLE 5 CHANGES AFTER ABSORPTION

FIGS. 2 and 3 are before and after Scanning Electron Microscopy (SEM) Images and x-ray diffraction patterns (XRD), respectively, for the SO<sub>2</sub> absorption by K<sub>x</sub>Mn<sub>8</sub>O<sub>16</sub> B at 325°C. As shown in FIG. 2, the morphology and the crystal structure of the K<sub>x</sub>Mn<sub>8</sub>O<sub>16</sub> material significantly changes after SO<sub>2</sub> absorption. The surface area of this

material also decreased sharply from 74 m<sup>2</sup>/g to 4.6 m<sup>2</sup>/g, and the XRD patterns indicate that the OMS structure had converted to a mixture of MnSO<sub>4</sub> and manganolangbeinite K<sub>2</sub>Mn<sub>2</sub>(SO<sub>4</sub>)<sub>3</sub>. A visible color change in the absorbent was also evident. It was initially black and changed to yellow after the SO<sub>2</sub> absorption.

5

#### EXAMPLE 6 TEMPERATURE DEPENDENCE

FIG 5 is a plot of the wt% of SO<sub>2</sub> absorption on K<sub>x</sub>Mn<sub>8</sub>O<sub>16</sub> B at 250°C, 325°C and  
10 475°C under the other test conditions as indicated in Table 1 (0.5 g 40-80 mesh absorbent, feed gas: 250 ppm SO<sub>2</sub>, 82% N<sub>2</sub>, 18% O<sub>2</sub>, ~ 8,000 hr<sup>-1</sup> GHSV). Even at as low a temperature as 250°C, this material could adsorb more than 66 wt% SO<sub>2</sub>, although absorption is not 100% and some SO<sub>2</sub> breakthrough was observed even initially.

15

#### EXAMPLE 7 FEED GAS FLOW RATE DEPENDENCE

FIG. 6 shows the feed gas GHSV effect on the SO<sub>2</sub> absorption on K<sub>x</sub>Mn<sub>8</sub>O<sub>16</sub> B at 325°C. The breakthrough SO<sub>2</sub> capacity decreased from 61, to 44, and 33 wt% as the feed  
20 GHSV increased from 8K, to 30K and 60K hr<sup>-1</sup>. As the feed GHSV increased, the total SO<sub>2</sub> absorption capacity decreased, but not significantly, from 74 to 64 and 63 wt%.

25

#### EXAMPLE 8 FEED GAS COMPOSITION DEPENDENCE

FIG. 7 shows that increasing SO<sub>2</sub> concentration in the feed gas from 50 ppm to 250 ppm almost had no effect on the SO<sub>2</sub> adsorption on K<sub>x</sub>Mn<sub>8</sub>O<sub>16</sub> B. FIG. 8 shows feed gas composition effect on the SO<sub>2</sub> absorption on K<sub>x</sub>Mn<sub>8</sub>O<sub>16</sub> B at 325°C. CO and NO, which also exist in the combustion waste gases, did not have any effect on the SO<sub>2</sub> absorption on K<sub>x</sub>Mn<sub>8</sub>O<sub>16</sub>. CO<sub>2</sub>, at ~ 13% level, could slightly, if any, decrease the SO<sub>2</sub> breakthrough capacity (from 61 wt% to 59wt% ) and the total SO<sub>2</sub> capacity (from 74 to 68 wt%).

Surprisingly, the OMS material K<sub>x</sub>Mn<sub>8</sub>O<sub>16</sub> B shows a higher SO<sub>2</sub> breakthrough capacity of 74 wt% and total SO<sub>2</sub> capacity of ~80 wt% in CO-NO-SO<sub>2</sub>-H<sub>2</sub>O mixture feed gas even through the GHSV was 17K hr<sup>-1</sup>. When steam was introduced into the system, the SCD signals were not very stable which may generate some error of the measurement. In the absent of O<sub>2</sub>, cryptomelane material K<sub>x</sub>Mn<sub>8</sub>O<sub>16</sub> B still has SO<sub>2</sub> breakthrough capacity of 41 wt% and total SO<sub>2</sub> capacity of 58 wt%. After SO<sub>2</sub> absorption test, the weight gain of the adsorbent was measured though it was not possible to collect all the adsorbent particles. Table 4 gives the weight gain data of the feed gas composition effect tests. For comparison, the total SO<sub>2</sub> absorption calculated from SO<sub>2</sub> concentration change for each test was also listed.

Table 4  
Adsorbent weight gain after SO<sub>2</sub> absorption test in different feed gas at 325°C

Feed Gas	Air	CO <sub>2</sub> effect	CO effect	NO effect	O <sub>2</sub> -free effect	CO-NO-H <sub>2</sub> O effect
Weight Gain, %	65.7	65.6	66.2	64	50	66.8
Total SO <sub>2</sub> absorbed, %	74.6	68.1	74.1	70.7	58	80.6

\* See Table 1 for detailed test conditions

### Discussion of Examples 1-8:

Based on reaction (1), the maximum SO<sub>2</sub> capacity is believed to be controlled by oxidation state of Mn in the adsorbent. For the OMS materials K<sub>x</sub>Mn<sub>8</sub>O<sub>16</sub> B and Cu-doped K<sub>x</sub>Mn<sub>8</sub>O<sub>16</sub> B, the average projected oxidation state of Mn is 4; there are very few K<sup>+</sup> cations present in the structure. If the small amount of K<sup>+</sup> is ignored, the maximum SO<sub>2</sub> capacity should be ~ 73.5 wt%. The measured maximum SO<sub>2</sub> capacities (see Tables 3 and 4) are ~ 70 wt% for these two materials, which is very close to 73.5 wt% and reflects the contribution of the K<sub>2</sub>O byproduct. This result supports the hypothesis that reaction (1) dominates SO<sub>2</sub> absorption. Direct evidence is also seen in the XRD patterns before and after the SO<sub>2</sub> absorption. After SO<sub>2</sub> absorption, the OMS structure completely changed to MnSO<sub>4</sub> and manganolangbeinite K<sub>2</sub>Mn<sub>2</sub>(SO<sub>4</sub>)<sub>3</sub>. The formation of K<sub>2</sub>Mn<sub>2</sub>(SO<sub>4</sub>)<sub>3</sub> means more SO<sub>4</sub><sup>2-</sup> than Mn<sup>2+</sup> is formed and that reaction (1) needs to be modified slightly. A postulate is that the cryptomelane material itself or the SO<sub>2</sub> adsorbed material (mostly MnSO<sub>4</sub>) acts as a catalyst for the following reaction and formation of K<sub>2</sub>Mn<sub>2</sub>(SO<sub>4</sub>)<sub>3</sub>.



Because the amount of K<sup>+</sup> is small, the whole SO<sub>2</sub> absorption process is mostly dominated by manganese oxidation. It should be noted that, while the presence of O<sub>2</sub> in

the feed gas does help increase absorption, it is not necessary, as demonstrated by the satisfactory absorption performance in the oxygen –free feed gas test (feed gas composition: 250 ppm SO<sub>2</sub>, 12.5% N<sub>2</sub>, and 87.5% He). After SO<sub>2</sub> absorption in an O<sub>2</sub>-free environment, both MnSO<sub>4</sub> and K<sub>2</sub>Mn<sub>2</sub>(SO<sub>4</sub>)<sub>3</sub> were formed, suggesting that other  
5 reactions involving oxygen transfer and formation of some amorphous phases also happened in an O<sub>2</sub>-free environment.

The synthesized K<sub>x</sub>Mn<sub>8</sub>O<sub>16</sub> A had an average projected Mn oxidation state of +3.5. The ideal formula for this material should be K<sub>4</sub>Mn<sub>8</sub>O<sub>16</sub> (after water removal at 500°C and assuming all the counter-cations are K<sup>+</sup>). Then according to reaction (1), the  
10 maximum capacity is 45wt%, which exactly matches the measurement (see Table 3). If reaction (2) also exists with this material, K<sub>2</sub>Mn<sub>2</sub>(SO<sub>4</sub>)<sub>3</sub> should form, which was not seen in an XRD pattern (not shown), and the maximum SO<sub>2</sub> capacity should be 60 wt%. This suggests that reaction (1) predominates, and that reaction (2) occurs only to a very small extent or not at all. Based on the results from K<sub>x</sub>Mn<sub>8</sub>O<sub>16</sub> A (hydrothermal synthesis, with  
15 projected final average Mn oxidation state 3.5), K<sub>x</sub>Mn<sub>8</sub>O<sub>16</sub> B (reflux synthesis, with projected final average Mn oxidation state 4) and Cu-doped K<sub>x</sub>Mn<sub>8</sub>O<sub>16</sub> B (hydrothermal synthesis, with projected final average Mn oxidation state 4), neither the choice between reflux or hydrothermal synthesis, nor doping with Cu significantly changes SO<sub>2</sub> break through absorption capacity or maximum absorption capacity. This suggests that there is  
20 no kinetic or thermodynamic effect attributable to doping or the synthesis mechanism.

The alternative synthesis method of purging  $O_2$  through a mixture of  $MnSO_4$  and KOH solution followed by calcination at  $600^\circ C$  did show some effect.  $K_xMn_8O_{16}$  C, synthesized using this method, gives  $\sim 50\text{wt}\%$   $SO_2$  breakthrough capacity and  $\sim 60\text{wt}\%$   $SO_2$  total capacity, which are lower than those for  $K_xMn_8O_{16}$  B. Potential reasons for this

5 disparity include 1) possible incomplete oxidation of  $Mn^{2+}$  to  $Mn^{4+}$ , 2) the relative low surface area ( $32\text{ m}^2/\text{g}$  vs.  $75\text{ m}^2/\text{g}$ ) and high density ( $\sim 1\text{ g}/\text{cm}^3$  vs.  $0.67\text{ g}/\text{cm}^3$ ), and 3) the product is not pure OMS as a small amount of  $K_2SO_4$  was found to exist (see Fig. 9 for its XRD pattern). While the synthesis conditions could still be optimized to improve adsorption performance, the absorption performance is adequate to be effective and

10 consideration of other factors renders this a desirable approach. For example, this synthesis method can significantly decrease the overall cost of the absorbent production. After  $SO_2$  absorption, almost pure  $MnSO_4$  is formed, which, being one of the starting materials, can be recaptured and reused. Also the density of  $K_xMn_8O_{16}$  C is  $\sim 50\%$  higher than that of  $K_xMn_8O_{16}$  B, which indicates more adsorbents can be loaded and

15 higher  $SO_2$  capacity in a given volume can be achieved.

Although electrolytic manganese dioxide (EMD) from Erachem Comilog, Inc. has  $Mn^{4+}$  and a surface area of  $\sim 30\text{ m}^2/\text{g}$ , the  $SO_2$  capacity for this material does not approach that of the OMS materials. This indicates that the OMS structure is important for high  $SO_2$  absorption.

20  $K_xMn_8O_{16}$  B was tested at a temperature  $250^\circ C$ ,  $325^\circ C$ , and  $475^\circ C$ . At  $250^\circ C$ , a lower  $SO_2$  absorption rate was observed but the maximum  $SO_2$  capacity is almost the

same as that measured at 325°C and 475°C. In comparing the results at 325°C and 475°C, minimal difference was observed except that at 475°C, after the breakthrough capacity was reached, the SCD detector background slightly increased, indicating that some SO<sub>3</sub> was being released even though total absorption amount was still increasing.

5           Substantial variation in the feed gas flow rate affected the SO<sub>2</sub> absorption performance of K<sub>x</sub>Mn<sub>8</sub>O<sub>16</sub> B adsorbent, though in practice this affect can be mitigated with appropriate sizing and design of the SO<sub>x</sub> trap. For example, the SO<sub>2</sub> breakthrough capacity decreased about 50% when the feed GHSV increased from 8K to 60K hr<sup>-1</sup>. This indicates the SO<sub>2</sub> absorption reaction is mostly controlled by SO<sub>2</sub> mass diffusion through  
10   the adsorbent. Since the SO<sub>2</sub> concentration in the feed gas had little or no effect on its absorption suggests that reaction (1) is 0<sup>th</sup> order for SO<sub>2</sub>, and it is mostly controlled by the available active sites on the adsorbent.

Most components in the simulated exhaust combustion gases tested, CO, NO, CO<sub>2</sub>, and H<sub>2</sub>O, did not have a significant effect on the SO<sub>2</sub> absorption capacity of the  
15   K<sub>x</sub>Mn<sub>8</sub>O<sub>16</sub> B adsorbent, and the absorption capacity in an oxygen free environment, while lower, was still acceptable. Therefore, it is expected that the Mn-OMS materials should be useful to remove SO<sub>2</sub> from gas streams in a wide variety of applications.

## EXAMPLE 9 OTHER OMS STRUCTURES

20

SO<sub>2</sub> absorption capacities of other manganese oxides with tunnel structure, including Todorokite-type magnesium manganese oxide with channels of 3 x 3 MnO<sub>6</sub>

units, sodium manganese oxide with channels of 2 x 4 MnO<sub>6</sub> units, sodium manganese oxide with channels of 2 x 3 MnO<sub>6</sub> units, and pyrolusite manganese oxide with 1 x 1 MnO<sub>6</sub> units, were studied.

Pyrolusite, MnO<sub>2</sub> 1 x 1, was obtained from Stream Chemicals. The as-received  
5 chemical was ball-milled for 1 hr to get ~ 1 μm particles before SO<sub>2</sub> absorption test. One todorokite material, OMS-1, was provided by Engelhard Corporation. Other tunnel-structured manganese oxides were prepared in the lab using the methods described in the published literatures.

Birnessite was used as precursor for the synthesis of channel-structured  
10 manganese oxides. Birnessite-type layered manganese oxides were prepared using the methods used by Golden, et al. (5) and (6). A typical synthesis was carried out as: 250 ml 6.4 M NaOH solution was mixed with 200 ml 0.5M MnSO<sub>4</sub> at room temperature. Oxygen was immediately bubbled through a glass frit at a rate of 4 L/min. After 4.5 h the oxygenation was stopped and the precipitate was filtered out and washed with  
15 deionized water 4 times, and then dried in air at 100°C. About 13 g grey color birnessite product was obtained.

Two sodium manganese oxides with channels of 2 x 3 MnO<sub>6</sub> units (Na 2 x 3 A & B) were prepared by directly calcination of birnessite in air for 12 h at 500°C, and 650°C, respectively. (7).

20 Todorokite (magnesium manganese oxide with channels of 3 x 3 MnO<sub>6</sub> units) was prepared as described in (5) and (8): ~3 g birnessite was added in 100 ml 1M



MgCl<sub>2</sub> solution, the mixture was shaken overnight at room temperature for Mg<sup>2+</sup> ion exchange for Na<sup>+</sup>. The slurry was washed four times with deionized water. Then, Mg<sup>2+</sup>-birnessite, together with 25 ml H<sub>2</sub>O, was autoclaved at 150°C for 48 hr. After washing with D.I water 3 times, the product was dried in air at 100°C. About 2.0 g todorokite-type tunnel structure manganese oxide (Mg 3 x 3) was obtained.

Sodium manganese oxide with channels of 2 x 4 MnO<sub>6</sub> units was prepared using method developed by Xia et al. (9). About 5 g birnessite, together with 25 ml 2.5M NaCl solution, was autoclaved at 210°C for 48 hr. After washing with D.I water 3 times, the product was dried in air at 100°C. About 4.4 g black color product, Na 2 x 4, was obtained.

The dried materials were sieved to provide 40 – 80 mesh particles for the SO<sub>2</sub> absorption test, which was carried out in a temperature controlled reactor with an the SCD analytical system. All these materials were tested under the same conditions (0.5 gram 40-80 mesh absorbent particles, 100 sccm feed flow of 250 ppm SO<sub>2</sub> in 82% N<sub>2</sub>, 18% O<sub>2</sub>) at a temperature of 325°C (See Table 5). Before each SO<sub>2</sub> absorption measurement, the absorbent material was heated at 500°C for 2 h in flowing air to remove residual moisture. To characterize the structure change before and after SO<sub>2</sub> absorption, powder X-ray diffraction pattern (XRD) was collected on some of the tested materials.

Table 5  
SO<sub>2</sub> absorption tests of other OMS materials

Absorbent	Test Conditions
MnO <sub>2</sub> 1 x 1 pyrolusite from Strem Chemicals, with 1 x 1 tunnels	0.5 g 40-80 mesh absorbent, 325°C, 100 sccm flow of 250 ppm SO <sub>2</sub> , 82% N <sub>2</sub> , 18% O <sub>2</sub> , GHSV = 18K hr <sup>-1</sup>
Na 2 x 3 A Na <sub>2</sub> Mn <sub>5</sub> O <sub>10</sub> , with 2 x 3 tunnels, calcined at 500°C for 12 h	0.5 g 40-80 mesh absorbent, 325°C, 100 sccm flow of 250 ppm SO <sub>2</sub> , 82% N <sub>2</sub> , 18% O <sub>2</sub> , GHSV = 3.4K hr <sup>-1</sup>
Na 2 x 3 B Na <sub>2</sub> Mn <sub>5</sub> O <sub>10</sub> , with 2 x 3 tunnels, calcined at 650°C for 12 h	0.5 g 40-80 mesh absorbent, 325°C, 100 sccm flow of 250 ppm SO <sub>2</sub> , 82% N <sub>2</sub> , 18% O <sub>2</sub> , GHSV = 5.1K hr <sup>-1</sup>
Na 2 x 3 A Na <sub>2</sub> Mn <sub>5</sub> O <sub>10</sub> , with 2 x 3 tunnels, calcined at 500°C for 12 h	0.5 g 40-80 mesh absorbent, 325°C, 100 sccm flow of 250 ppm SO <sub>2</sub> , 82% N <sub>2</sub> , 18% O <sub>2</sub> , GHSV = 11K hr <sup>-1</sup>
Na 2 x 4 sodium manganese oxide with 2 x 4 tunnels	0.5 g 40-80 mesh absorbent, 325°C, 100 sccm flow of 250 ppm SO <sub>2</sub> , 82% N <sub>2</sub> , 18% O <sub>2</sub> , GHSV = 11K hr <sup>-1</sup>
OMS-1 todorokite, with 3 x 3 tunnels, provided by Engelhard Corporation	0.5 g 40-80 mesh absorbent, 325°C, 100 sccm flow of 250 ppm SO <sub>2</sub> , 82% N <sub>2</sub> , 18% O <sub>2</sub> , GHSV = 11K hr <sup>-1</sup>
Mg 3 x 3 Todorokite, with 3 x 3 tunnels Synthesized	0.5 g 40-80 mesh absorbent, 325°C, 100 sccm flow of 250 ppm SO <sub>2</sub> , 82% N <sub>2</sub> , 18% O <sub>2</sub> , GHSV = 2.7 hr <sup>-1</sup>

\* Before each SO<sub>2</sub> absorption measurement, the absorbent material was heated at 500°C for 2 h in 100 sccm air.

#### EXAMPLE 10 OTHER OMS STRUCTURES RESULTS AND COMPARISON

10           The measured breakthrough capacities at selected gas flow rates for the materials prepared in Example 9 are given in Table 6 along with exemplary capacities for the 2x2 structure of Example 1.

**Table 6**  
**SO<sub>2</sub> absorption capacity of OMS absorbents**

Material tested	GHSV, hr <sup>-1</sup>	Break through capacity, wt%
MnO <sub>2</sub> , from Strem Chemicals, 1 x 1 tunnels of MnO <sub>6</sub> units	18K	<0.1
Na <sub>2</sub> Mn <sub>5</sub> O <sub>10</sub> , 2 x 3 tunnels of MnO <sub>6</sub> units, calcined at 500°C for 12 h (A)	3.4K	57.5
Na <sub>2</sub> Mn <sub>5</sub> O <sub>10</sub> , 2 x 3 tunnels of MnO <sub>6</sub> units, calcined at 650°C for 12 h (B)	5.1K	31
Na <sub>2</sub> Mn <sub>5</sub> O <sub>10</sub> , 2 x 3 tunnels of MnO <sub>6</sub> units, calcined at 500°C for 12 h (A)	11K	12
Sodium Manganese Oxide, 2 x 4 tunnels of MnO <sub>6</sub> units	11K	33
MgMn <sub>2</sub> O <sub>4</sub> from todorokite (3x3) provided by Engelhard Corporation	11K	1.5
MgMn <sub>2</sub> O <sub>4</sub> from the synthesized todorokite (3x3)	2.7K	53
Cryptomelane, 2 x 2 tunnels of MnO <sub>6</sub> units	8K	62
Cryptomelane, 2 x 2 tunnels of MnO <sub>6</sub> units	30K	42

- 5            Save two of the materials, the SO<sub>2</sub> breakthrough absorption capacities for these materials are generally much higher than those of conventional SO<sub>x</sub> absorbents (normally

less than 5 wt%), establishing their usefulness as SO<sub>x</sub> absorbents pursuant to the present invention.

The 1x1 MnO<sub>2</sub> from Strem Chemicals was confirmed by XRD to be well crystallized pyrolusite, which consists of 1 x 1 MnO<sub>6</sub> tunnels. After calcination at 500°C for 2 h in air, the structure remained stable. However the material exhibits poor absorption capacity, with a breakthrough capacity of about 0.1% and a maximum absorption capacity less than 3%.

The birnessite synthesized in this work was calcined in air either at 500°C for 12 h (A), or at 650°C for 12h (B). In either case, sodium manganese oxide, Na<sub>2</sub>Mn<sub>5</sub>O<sub>10</sub>, forms, the basic structure which consists of MnO<sub>6</sub> octahedra joined at edges to form a 2 x 3 tunnel structure. (7) FIG. 8 shows the SO<sub>2</sub> absorption performance of both the A and B formulations of this microporous manganese oxide under different GHSV. Similar to the 2x2 cryptomelane materials, this microporous manganese oxide also has very high SO<sub>2</sub> absorption capacity. At 3444 hr<sup>-1</sup> GHSV, the total SO<sub>2</sub> absorbed is ~ 70 wt%. At higher GHSV, the SO<sub>2</sub> absorption performance decreases, indicating the reaction is controlled by the mass diffusion of SO<sub>2</sub> through the absorbent. After SO<sub>2</sub> absorption, MnSO<sub>4</sub> forms.

The XRD pattern of the sodium manganese oxide synthesized by hydrothermal reaction in this work matched very well with the XRD pattern of the sodium manganese oxide material with 2 x 4 tunnel structure published by Xia et al. (10) Likewise, as expected, after calcination at 500°C for 12 h in air, the 2 x 4 tunnel structure remains

unchanged. FIG 9 gives the SO<sub>2</sub> absorption test result at 10755 hr<sup>-1</sup> GHSV. This material also has high SO<sub>2</sub> absorption capacity.

While the todorokite magnesium manganese oxide prepared by hydrothermal reaction in this work was not well crystallized, the todorokite structure could still be identified in the XRD. However, after calcination at 500°C for 2 h in air, the 3 x 3 tunnel structure changed mostly to MgMn<sub>2</sub>O<sub>4</sub>. This structure change was evident in the MgMn<sub>2</sub>O<sub>4</sub> provided by Engelhard Corporation as well. While the todorokite materials both exhibited relative high absorption capacities, this instability at moderately high temperatures is a relative disadvantage for most applications. While the could be used as absorbents, most conventional implementations require stability above the absorbents at 500°C or sometimes higher.

## CLOSURE

While the invention has been illustrated and described in detail in the drawings and foregoing description, the same is to be considered as illustrative and not restrictive in character. Only certain embodiments have been shown and described, and all changes, equivalents, and modifications that come within the spirit of the invention described herein are desired to be protected. Any experiments, experimental examples, or experimental results provided herein are intended to be illustrative of the present invention and should not be considered limiting or restrictive with regard to the invention scope. Further, any theory, mechanism of operation, proof, or finding stated herein is

meant to further enhance understanding of the present invention and is not intended to limit the present invention in any way to such theory, mechanism of operation, proof, or finding. Thus, the specifics of this description and the attached drawings should not be interpreted to limit the scope of this invention to the specifics thereof. Rather, the scope  
5 of this invention should be evaluated with reference to the claims appended hereto. In reading the claims it is intended that when words such as “a”, “an”, “at least one”, and “at least a portion” are used there is no intention to limit the claims to only one item unless specifically stated to the contrary in the claims. Further, when the language “at least a portion” and/or “a portion” is used, the claims may include a portion and/or the entire  
10 items unless specifically stated to the contrary. Likewise, where the term “input” or “output” is used in connection with a fluid processing unit, it should be understood to comprehend singular or plural and one or more fluid channels as appropriate in the context. Finally, all publications, patents, and patent applications cited in this specification are herein incorporated by reference to the extent not inconsistent with the  
15 present disclosure as if each were specifically and individually indicated to be incorporated by reference and set forth in its entirety herein, including the following scientific publications referenced in the specification above:

(1) X. Chen, Y.F. Shen, S. L. Suib, and C.L. O’Young, “Characterization of  
20 Manganese Oxide Octahedral Molecular Sieve (M-OMS-2) Materials with Different Metal Cation Dopants”, *Chem. Mater.* **2002**, *14*, 940-948.

- (2) G.G. Xia, Y.G. Yin, W.S. Willis, J.Y. Wang, and S.L. Suib, "Efficient Stable Catalysts for Low Temperature Carbon Monoxide Oxidation", *J. Catal.* **1999**, *185*, 91-105.
- (3) R.N. DeGuzman, Y.F. Shen, E.J. Neth, S.L. Suib, C.K. O'Young, S. Levine,  
5 and J.M. Newsam, "Synthesis and Characterization of Octahedral Molecular Sieves (OMS-2) Having the Hollandite Structure", *Chem. Mater.* **1994**, *6* 815-821.
- (4) S. L. Suib, C-L O'Young, "Synthesis of Porous Materials", M. L. Occelli, H. Kessler, eds, M. Dekker, Inc., p. 215, 1997.
- (5) D.C. Golden, C.C. Chen, and J.B. Dixon, "Synthesis of Todorokite", *Science*,  
10 **1986**, *231*, 717-719.
- (6) D.C. Golden, C.C. Chen, and J.B. Dixon, "Transformation of birnessite to buserite, todorokite, and manganite under mild hydrothermal treatment", *Clays Clay Miner.* **1987**, *35*, 271-280.
- (7) J.P. Parant, R. Olazcuaga, M. Devalette, C. Fouassier, and P. Hagenmuller,  
15 "Sur Quelques Nouvelles Phases de Formule  $\text{Na}_x\text{MnO}_2$  ( $x \leq 1$ )", *J. Solid State Chem.* **1971**, *3*, 1-11.
- (8) Y.F. Shen, R.P. Zerger, R.N. DeGuzman, S.L. Suib, L. McCurdy, D.I. Potter, and C.L. O'Young, "Manganese oxide octahedral molecular sieves: preparation, characterization, and applications", *Science*, **1993**, *260*, 511-515

(9) G.G. Xia, W. Tong, E.N. Tolentino, N.G. Duan, S.L. Brock, J.Y. Wang, S.L. Suib, and T. Ressler, “ Synthesis and characterization of nanofibrous sodium manganese oxide with a 2 x 4 tunnel structure”, *Chem. Mater*, **2001**, 13, 1585-1592.